

# Ab initio GW electron-electron interaction effects in Quantum Transport

Pierre Darancet,<sup>1,2</sup> Andrea Ferretti,<sup>3,2</sup> Didier Mayou,<sup>1,2</sup> and Valerio Olevano<sup>1,2</sup>

<sup>1</sup>LEPES, UPR 11 CNRS, 38042 Grenoble, France

<sup>2</sup>European Theoretical Spectroscopy Facility (ETSF)

<sup>3</sup>Dipartimento di Fisica, Università di Modena e Reggio Emilia, and INFN-CNR-S3,  
National Center on nanoStructures and bioSystem s at Surfaces, 41100 Modena, Italy

(Dated: March 23, 2024)

We present an ab initio approach to electronic transport in nanoscale systems which includes electronic correlations through the GW approximation. With respect to Landauer approaches based on density-functional theory (DFT), we introduce a physical quasiparticle electronic-structure into a non-equilibrium Green's function theory framework. We use an equilibrium non-selfconsistent  $G^0W^0$  self-energy considering both full non-hermiticity and dynamical effects. The method is applied to a real system, a gold mono-atomic chain. With respect to DFT results, the conductance profile is modified and reduced by the introduction of diffusion and loss-of-coherence effects. The linear response conductance characteristic appear to be in agreement with experimental results.

PACS numbers: 72.10.Dj, 71.10.-w, 72.15.Nj, 73.63.-b

Electronics at the nanoscale, namely nanoelectronics, represents the next years' technological challenge. It is boosted not only by the need for shorter integration scales, but also by the expectation that unusual quantum effects [1] are going to be observed due to quantum phenomena effects. Beside the experimental efforts to synthesize nanoelectronic devices, quantum transport theory [2] has the formidable task to understand and to model the mechanisms behind these phenomena and to predict them from a first principles approach.

In the last years, a combination of ab initio density-functional theory (DFT) calculations together with the description of transport properties in a Landauer-Buttiker (LB) framework [2] has demonstrated its ability to describe small bias coherent transport in nanojunctions [3, 4, 5]. These approaches were successful in accounting for the contact resistance and conductance degrading mechanisms induced by impurities, defects and non-commensurability patterns in the conductor region. The major objections raised to such method are: (i) the Kohn-Sham (KS) electronic structure is in principle unphysical, to be considered only as an approximation to the quasiparticle (QP) electronic structure; (ii) non-coherent and dissipative effects due to electron-phonon (e-ph) and electron-electron (e-e) scattering can be taken into account only approximatively in the LB formalism; (iii) non-linear response and far from equilibrium none-bias transport are not accessible, since DFT cannot be applied to open systems and is not a non-equilibrium theory (although recent works [6] have demonstrated that time-dependent DFT can tackle the problem).

Non-equilibrium Green's function (NEGF) theory [7, 8] is in principle a correct approach to address the above objections. The critical point within this theory is the choice of good approximations to the self-energy  $\Sigma$ , and coherently to the scattering functions  $G^< >$ . This ensures that both the renormalization of the QP energies

and the electron diffusion mechanisms due e.g. to e-ph or e-e interactions will be properly taken into account. First works studying the role of the e-ph coupling [9, 10] and of short-range e-e correlations [11, 12] or the renormalization of the QP energies [13] have recently appeared in the literature, or, we are aware, are going to appear [14]. The role of correlations, apart from being central in explaining e.g. Coulomb blockade and Kondo effects, could also be crucial in bridging the gap between experimentally-observed and LB-predicted conductances, in some cases are orders of magnitude off [6, 12, 15].

In this work, we introduce electronic correlations in the calculation of transport by an ab initio approach based on Hedin's GW approximation (GWA) [16, 17] in the framework of NEGF. In our scheme, the GW self-energy is built at equilibrium and the Green's function is calculated by direct solution of the Dyson equation. For the lead/conductor/lead geometry, the GW self-energy is summed to the lead's self-energies; the electronic conductance is calculated through the Meir-Wingreen formula [19], a NEGF Landauer-like expression derived for interacting conductors. We apply this scheme to a realistic system, a gold mono-atomic unidimensional chain [20], and we study the effects induced on transport properties by the different components of the GW self-energy, the hermitean and the non-hermitean parts and the dynamical dependence. Our results show that the conductance profile is considerably modified by the real part of the GW correction. The imaginary part introduces a suppression of the conductance, which is negligible close to the Fermi energy, but that increases with the energy. Finally, the full dynamical dependence of the GW self-energy introduces further structures far from the Fermi energy, which have to be ascribed to satellite excitations of the system. The GW smooth drop on the conductance characteristics as a function of the bias at very low voltage compares favorably with the trend

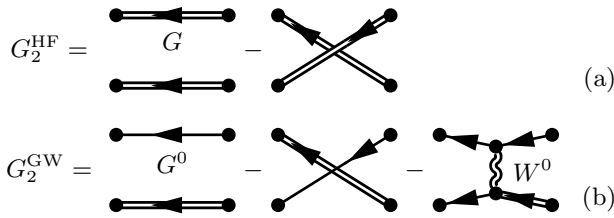


FIG. 1: 2-particle Green's function in the self-consistent Hartree-Fock (a) and in the non self-consistent  $G^0W^0$  approximation (b). Thin line: non self-consistent  $G^0$ ; double line: self-consistent  $G$ ; wiggly line: RPA non self-consistent  $W^0$ .

experimentally measured in gold nanowires [20].

With respect to Hartree-Fock (HF), which already renormalizes the energies for the e-e classical repulsion and exchange, the GWA introduces the important contribution due to correlations and to e-e scattering diffusion mechanisms responsible for loss-of-coherence in transport. Indeed, by direct inspection of the diagrammatic representation of the 2-particle Green's function  $G_2$  (see Fig. 1 and Refs. [7, 18]), one can see that the  $G_2^{HF}$  describes an uncorrelated propagation and that collisional terms are missing. This implies that the HF scattering functions,  $< \dots >$  and  $> \dots <$ , are exactly zero. On the other hand, even a non-selfconsistent  $G^0W^0$  approximation introduces a collisional term [the last diagram in Fig. 1(b)] which gives rise to non-zero  $< \dots >$ , and in turn to e-e scattering mechanisms and incoherent, dissipative effects in transport. As it is shown by the corresponding  $G_2$  Feynman diagram, the  $G^0W^0$  approximation is not a conserving approximation in the Baym and Kadanoff sense [7], leading to, e.g., non conservation of the number of particles. However, the relative deviation from the exact density brought by the  $G^0W^0$  approximation has been evaluated by Schindlmayr et al. [18] to be only of the order of 0.05% for the range of metallic densities ( $r_s^Au = 3.01$ ) of interest here.

Our starting point is a standard DFT-LDA calculation based on plane waves (PWs) and norm-conserving pseudopotentials for an infinite mono-atomic chain of gold atoms using periodic boundary conditions [21]. The KS electronic structure is calculated both at the relaxed atomic distance (4.72 Bohr) and in a stretched geometry (5.32 Bohr), so as to simulate the experimental situation described in Ref. [20] (conductance measures of a gold monoatomic chain pulled up from a gold surface by an STM tip) and also the calculations reported in Ref. [9]. From the DFT KS eigenfunctions, we obtain an orthonormal set of maximally localized Wannier functions (MLWF) [22], which are used as a basis set in the calculation of quantum transport. The following step is a converged [23] GW plane-wave calculation of both the QP energies and the self-energy matrix elements for the six bands around the Fermi energy, corresponding to the

gold sd-m manifold. The self-energy in the  $G^0W^0$  approximation at equilibrium is given by:

$$\Sigma^{GW}(\omega) = \frac{i}{2} \int_{-\infty}^{\infty} d\omega' e^{i(\omega - \omega')\tau} G^0(\omega') W^0(\omega - \omega'); \quad (1)$$

where  $G^0$  is the Green's function built on the non-interacting KS electronic structure and  $W^0$  is the dynamically screened interaction given by the RPA polarizability,  $P^{RPA} = iG^0G^0$ . Since for transport we need a  $\omega$ -grid fully dynamical dependence of the self-energy, we calculate the frequency integral of Eq. (1) in three different ways: (i) by approximating the dynamical dependence of  $W^0(\omega)$  through a plasmon-pole (PP) model [17]; (ii) by a contour deformation (CD) method [24], which consists in a deformation of the real axis contour such that the self-energy can be calculated as an integral along the imaginary axis minus a contribution arising from the residual of the contour-included poles of  $G$ ; (iii) by an analytic continuation (AC) method [25], i.e. calculating the integral and also the self-energy on the imaginary axis and then performing an analytical continuation to the real axis. In the last step we carried out the quantum transport calculation using a modified version of the WAnT code [3, 11]. We first projected the GW self-energy, as well as the non-interacting hamiltonian  $H^0$ , on the Wannier functions basis set (non-diagonal self-energy elements in the Bloch basis were neglected). We study the bulk conductance and also partition the system into three regions: the right (R) and left (L) leads (two semi-infinite gold mono-atomic chains) and a central (C) region, constituted by a single gold atom. This has the purpose of clarifying the role of both intra-conductor and conductor-lead correlations. We calculate the retarded Green's function in the space spanned by the MLWF set by inverting the Dyson equation, i.e.

$$G^r(\omega) = [H^0 - \Sigma^r(\omega)]^{-1} \quad (2)$$

where  $H^0$  is the KS hamiltonian once the exchange-correlation contribution is subtracted,  $H^0 = H_{KS} - V_{xc}$ . For the tri-partitioned geometry, the total retarded self-energy,

$$\Sigma^r = \Sigma_L^r + \Sigma_R^r + \Sigma_{GW}^r; \quad (3)$$

is the sum of the correlation GW and lead self-energies. The conductance is finally calculated using the following formula:

$$C(\omega) = \frac{2e^2}{h} \text{tr}[G^a \Sigma_R^r G^r \Sigma_L^r (\Sigma_L^r + \Sigma_R^r)^{-1}]; \quad (4)$$

first given by Meir and Wingreen [19] and recently re-derived under more general conditions [11]. Here  $\Sigma = \Sigma_L + \Sigma_R + \Sigma_{GW}$ , not to be confused with the vertex function, is the total decay rate (the sum of the electron in-

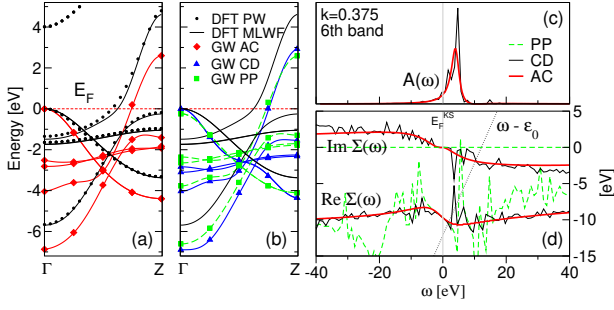


FIG. 2: (color online) (a) and (b): DFT-LDA Kohn-Sham vs GW electronic structure: black dots: DFT-LDA on PW basis; lines: DFT-LDA on MLWF; squares, triangles and diamonds refer to GW calculations from the PP model, the CD, and the AC methods respectively. Fermi energy is set to zero. (c) Spectral function and (d) real and imaginary part of the GW self-energy: dashed, thin and thick lines are from the PP model, the CD, and the AC methods respectively. The dotted curve is the straight line  $\epsilon_F^{\text{KS}} + \hbar v_{\text{FC}}$  whose intersections with the real part of the self-energy give the peaks of the spectral function. The 0 is set to the Kohn-Sham Fermi energy.

and out-scattering functions), due to both the presence of the R and L leads and the effect of the e-e interaction,

$$= i(\epsilon^{\text{r}} - \epsilon^{\text{a}}) = i(\epsilon^{\text{r}} - \epsilon^{\text{a}}); \quad (5)$$

With respect to the Landauer formula, Eq. (4) presents a factor  $(\epsilon_L + \epsilon_R)^{-1}$  which reduces to one in the uncorrelated case. Equation (4) represents an effective (including correlation effects) transmission probability of an electron injected at energy  $\epsilon$  through the conductor.

In Fig. 2(a,b) we compare the DFT-LDA (Kohn-Sham) and the GW (quasiparticle) electronic structure for the relaxed geometry. The dots represent the DFT-LDA levels from the PW calculation. We verified that the diagonalization on the MLWF basis (solid lines) closely reproduces the PW results. Squares, triangles, and diamonds represent the GW electronic structures calculated using the PP model, the CD, and the AC methods, respectively. Little difference among the GW methods is found. The GW corrections globally lower the d-like states with the Fermi level, and also reduce the s-like bandwidth (this effect is less evident in the stretched chain where the bandwidth shrinks about 3 eV already at the DFT level).

In Fig. 2, we compare the real and imaginary parts of the self-energy (d) and the spectral function  $A = i(G^{\text{r}} - G^{\text{a}})$  (c) for a point close to the Fermi level. We remark that the AC method appears to smooth the richer-in-structure CD spectrum. Although computationally cheaper, the AC method should be considered less accurate than CD, especially on the imaginary part. However, the frequency dependence as well as the shape and the position of the main structures (both QP and satellites peaks) are essentially caught by both methods. There-

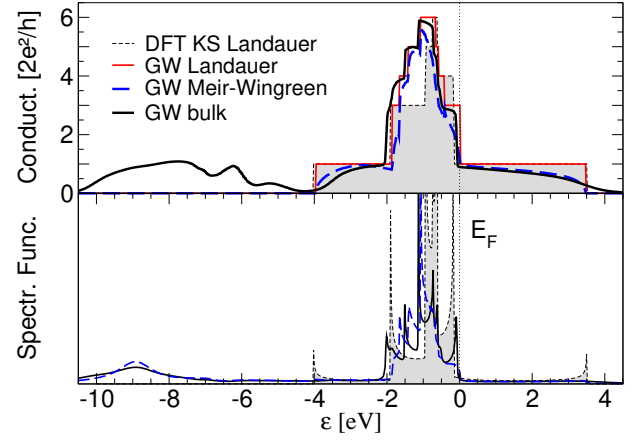


FIG. 3: (color online) Conductance (top) and spectral function (bottom) for the stretched atomic configuration. The Fermi level is set to zero. Thin dashed line: Landauer result using a DFT KS structure; thin solid line: Landauer using only a real part GW renormalization of the energies; thick dashed line: Meir-Wingreen result using GW realpart renormalization in the leads and a full (hermitean+antihermitean) dynamical GW self-energy in the conductor; thick solid line: GW bulk conductance with full dynamical self-energy.

fore, we use the AC approach in the following.

In Fig. 3 we show the conductance and the spectral function of the gold chain for the stretched geometry, obtained using different methods: The thin dashed line is calculated using the Landauer formula and the DFT KS electronic structure. The conductance at the Fermi level for the stretched chain appears to be one (in units of  $2e^2/h$ ) and it is of s-like character. This is true also for the relaxed structure (not shown), although in that case the Fermi level is at the limit of the onset of the d-like states. The thin solid line is obtained from the Landauer formula evaluated using the GW real-part-only QP energies. GW corrections are considered both in the conductor and in the leads. Otherwise, a fictitious contact resistance, unphysical for a homogeneous system, would appear. At this first level, the net effect is a renormalization of KS into QP energies, the true energies to introduce and remove an electron from the system. Therefore, the GWA affects the conductance profile by modifying the position of the conductance steps, especially in the d-like region. In the relaxed geometry, the GWA also narrows the s-like conductance channel.

The thick dashed line in Fig. 3 represents the result obtained in the tri-partitioned geometry by using the Meir-Wingreen formula and introducing a full non-hermitean and dynamical GW self-energy in the conductor. Static real-part-only QP energies are included in the leads. This introduces loss-of-coherence only in the conductor while leaving the leads ballistic. At the same time it limits the introduction of fictitious contact resistances, i.e. the QP levels are aligned in the leads and the conductor.

The difference of this curve wrt the thin solid line genuinely represents the effect of e-e scattering mechanisms in the conductor, causing diffusion, loss of coherence and appearance of resistance. With respect to Landauer approaches, the spectral function now appears as a collection of broadened QP peaks, whose finite width is directly associated to the inverse of the electronic lifetime of the QP state. The spectral weight, which is spread out, results in a lowering and a spill-out of the conductance step-like profile. This effect is directly related to the imaginary part of the QP energies, and can be seen to increase with  $E_F$  although not with a quadratical scaling Fermi-liquid behaviour, as it is normally observed in GW results for 3D systems. Finally, we calculate the fully correlated bulk GW conductance by taking into account a non-hermitian and dynamical GW self-energy everywhere in the system, conductor and leads (thick solid line). With respect to the previous case, even residual contact resistances (due to the fact that the conductor and leads spectral peaks were differently shaped, with finite and in infinitesimal widths respectively) are completely removed, and the conductance increases almost overall. Only around 3 eV we see a slight drop, which is due to the specific  $(L + R)^{-1}$  factor in Eq. (4). Moreover, new structures appear in the conductance at the lowest energies. By inspecting the spectral function, we can attribute them to the presence of satellites of electronic origin, i.e. plasmons or shake-ups, of the main QP peaks. Since the e-e interaction is an elastic scattering mechanism, these satellites are necessary to balance the losses which occur at energies close to the Fermi level, and are therefore important for transport. The e-e scattering acts in a way to redistribute the conductance channels to different energies, rather than globally destroy conductance as in the e-ph scattering, where momentum and current is lost to ionic degrees of freedom.

Taking the GW bulk result, we have integrated the conductance curve such to obtain the voltage characteristics of the correlated system. We compare with the experimental results of Ref. [20] and the e-ph result of Ref. [9], calculated at exactly the same stretched 5.35 Bohr interatomic distance. Like in that work, we assume that an equilibrium picture can still be appropriate to describe the small voltage range of 30 mV. The GW result is shown in Fig. 4 (dots). The results from Ref. [9] attribute the step in the conductance, occurring at 15 mV, to the onset of phononic processes. Instead, the continuous drop observed in our electronic correlated conductance, occurring in the first 15 mV, compares favorably with the drop observed experimentally [20]: e-e scattering mechanisms seem hence responsible for the conductance drops at very low bias. While the quantitative agreement with the experiment on the conductance value may be somewhat fortuitous [27], the trend in this drop is a direct consequence of the increase in the GW imaginary part of QP energies.

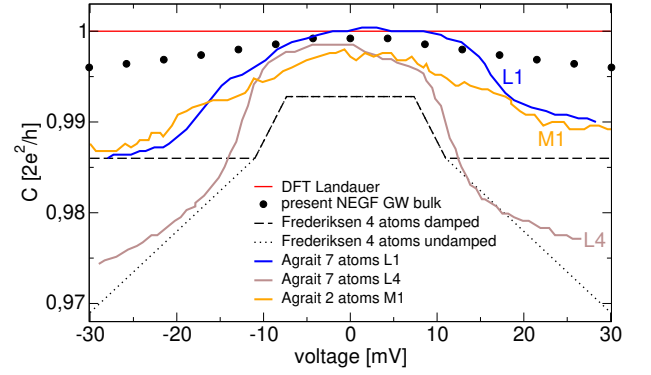


FIG. 4: (color online) Differential conductance vs applied bias. Thin solid line: DFT Landauer result; dots: present NEGF GW bulk result for the 5.35 Bohr interatomic distance; dashed and dotted line: e-ph theory of Ref. [9] corresponding to 4 atoms, same interatomic distance and for the damped and undamped limits; thick solid lines: experimental result of Ref. [20] corresponding to 2 and 7 atoms and different chain strains.

In conclusion, we have calculated the conductance of a realistic gold chain system by taking into account e-e correlation effects within the GW approximation. With respect to Landauer DFT results, the conductance profile is considerably modified. Already at the level of an equilibrium non-self-consistent GW, the trend of the differential conductance appears to compare favorably with the trend experimentally observed for this system.

We thank L. Reining, D. Feinberg, H. Mera, M. Verstraete, Y. M. Niquet and E. Shirley for useful discussions and remarks. Computer time has been granted by IDRIS proj. 060932. AF acknowledges funding by Italian MIUR through PRIN 2004.

- 
- [1] J. Park et al., *Nature* 417, 722 (2002); P. Jarillo-Herrero et al., *Nature* 434, 484 (2005); Z. Yao, H. Postma, L. Balents, and C. Dekker, *Nature* 402, 273 (1999).
  - [2] S. Datta, *Electronic Transport in Mesoscopic Systems*, Cambridge University Press, New York, 1995.
  - [3] A. Calzolari, N. Marzari, I. Souza, and M. B. Nardelli, *Phys. Rev. B*, 69, 035108 (2004).
  - [4] M. Brandbyge, J. L. Mozos, P. Ordejón, J. Taylor and K. Stokbro, *Phys. Rev. B*, 65, 165401, (2002); J. J. Palacios, A. J. Perez-Jimenez, E. Louis, E. SanFabian and J. A. Verges, *Phys. Rev. Lett.*, 90, 106801 (2003).
  - [5] S. Latil, S. Roche, D. Mayou, and J.-C. Charlier, *Phys. Rev. Lett.* 92, 256805 (2004); F. Triozon, S. Roche, A. Rubio, and D. Mayou, *Phys. Rev. B* 69, 121410 (R) (2004).
  - [6] S. Kurth, G. Stefanucci, C. O. Almbladh, A. Rubio and E. K. U. Gross, *Phys. Rev. B*, 72, 035308 (2005).
  - [7] L. P. Kadanoff and G. Baym, *Quantum Statistical Mechanics*, Benjamin, New York, 1962.
  - [8] H. Haug and A.-P. Jauho, *Quantum kinetics in transport*

- and optics of semiconductors, Springer, Berlin, 1996.
- [9] T. Frederiksen, M. Brandbyge, N. Lorente, and A. P. Jauho, *Phys. Rev. Lett.*, **93**, 256601 (2004).
  - [10] N. Sergueev, D. Roubtsov, and H. Guo, *Phys. Rev. Lett.*, **95**, 146803 (2005).
  - [11] A. Ferretti et al., *Phys. Rev. Lett.*, **94**, 116802 (2005); A. Ferretti, A. Calzolari, R. Di Felice and F. Manghi, *Phys. Rev. B*, **72**, 125114 (2005).
  - [12] P. Delaney and J. C. Greer, *Phys. Rev. Lett.*, **93**, 036805 (2004).
  - [13] A. Pecchia et al., *J. Comp. Electronics*, **4**, 79 (2005).
  - [14] K. S. Thygesen and A. Rubio, submitted.
  - [15] F. Evers, F. Weigend and M. Koentopp, *Phys. Rev. B*, **69**, 235411 (2004).
  - [16] L. Hedin, *Phys. Rev.* **139**, 796 (1965).
  - [17] M. S. Hybertsen and S. G. Louie, *Phys. Rev. Lett.*, **55**, 1418 (1985); R. W. Godby and R. J. Needs, *Phys. Rev. Lett.*, **62**, 1169 (1989).
  - [18] A. Schindlmayr, P. Garcia-Gonzalez and R. W. Godby, *Phys. Rev. B*, **64**, 235106 (2001).
  - [19] Eq. (10) in Y. Meir and N. S. Wingreen, *Phys. Rev. Lett.*, **68**, 2512 (1992).
  - [20] N. Agrat, C. Untiedt, G. Rubio-Bollinger and S. Vieira, *Phys. Rev. Lett.*, **88**, 216803 (2002).
  - [21] Gold 6s and 5d electrons are kept in valence. We adopt a cutoff of 30 Ry for wavefunctions and a (8;1;1) k-grid.
  - [22] N. Marzari and D. Vanderbilt, *Phys. Rev. B*, **56**, 12847 (1997).
  - [23] We used 150 and 100 states to converge  $W$  and  $\epsilon$  respectively; 2503 plane waves have been used to represent the wavefunctions and  $\epsilon$ , while the dimension of the  $\epsilon$  and  $W$  reciprocal-space matrices was 49. Imaginary axis integrations were carried out by a Gauss quadrature using 30 nodes. In the analytical continuation, we used a Padé approximant on 12 nodes. We used a modified version of the ABINIT code.
  - [24] A. Fleszar and W. Hanke, *Phys. Rev. B*, **56**, 10228 (1997).
  - [25] H. N. Rojas, R. W. Godby and R. J. Needs, *Phys. Rev. Lett.*, **74**, 1827 (1995).
  - [26] G. M. Rignanese, X. Blase and S. G. Louie, *Phys. Rev. Lett.*, **86**, 2110 (2001).
  - [27] In general GW does not achieve such levels of accuracy.